Published in Journal of Rock Mechanics and Tunneling Technology, 2004, Vol 10, No 1, P 31-47

DEVELOPMENT OF PREDICTIVE MODELS FOR CONTROLLING BLAST-INDUCED OVERBREAK IN TUNNELS

V.M.S.R. Murthy
and **Kaushik Dey**
Department of Mining Engineering,
Indian School of Mines, Dhanbad –826 004,
Telefax: (0326) 2206396 (O)
vmsr_murthy@yahoo.com

ABSTRACT

Drilling and blasting continues to be the predominant rock excavation technique in driving horizontal openings and tunnels for underground construction purpose. Faster drivages, attempted these days for reducing the long gestation periods of projects, have often resulted in large overbreak. This is due to the unacceptable levels of ground vibration to which the rock is subjected. Factors contributing to this include longer pulls; burn cuts, higher explosive per hole and per delay etc. Blast-induced rock damage (BIRD) assessment based on far-field peak particle velocity (PPV) measurement, when extrapolated near the face, has often resulted in suggesting higher PPV threshold levels. Apart from this the geological and structural features play a dominant role in masking the intensity of blast waves. Therefore, near-filed monitoring using accelerometers has been attempted in one of the metal mines to study the blast damage in faces excavated by burn cut. Present seismographs available have limited range (2540mm/s) and are not suitable for near-field monitoring. This paper reports the investigations carried out for measuring acceleration, PPV and overbreak in a development heading for arriving at a suitable method of predicting blast-induced rock damage. The analysis of both acceleration and PPV measured against overbreak has revealed that rock damage is found to depend more on acceleration than PPV.

KEY WORDS: *Tunnels, blast-induced overbreak, acceleration, peak particle velocity, threshold levels*

1.0 INTRODUCTION

Underground construction for mining as well as for civil engineering projects requires driving of drifts and tunnels in a large number. In recent years, mechanical excavation with drifting and tunneling rigs (Road headers, TBMs) has advanced considerably, excavating rocks with compressive strengths up to 250 MPa. However, excavation with explosives is still widely accepted technique as the mechanical cutting has its inconveniences due to rigid work system (as the sections must be circular), ground to be excavated must not have important variations or geological upsets, curves should have a radius over 300 m, initial excavation is costly and personnel must be highly specialized.

Excavation with drilling and blasting solves most of these problems but is seriously affected by poor drivage rate. Attempts to get longer pull, which is associated with use of higher explosive charge per hole and per delay as well, leads to roof rock damage. In order to control and reduce blast-induced rock damage, assessment of the extent of damage is a prerequisite. Most of the existing criteria relate damage to ground vibrations resulting from dynamic stresses induced by the blasting process. An attempt has been made to monitor the blast-induced accelerations and PPV simultaneously to arrive at predictive models for controlling overbreak.

2.0 BLAST DAMAGE ASSESSMENT

Explosive charge when detonated crushes the rock immediately surrounding the blasthole. The extent of the crushed zone is influenced by the magnitude of the explosion relative to dynamic compressive breaking strength (σ_{cd}) of the rock and also by the degree of coupling (the ratio of cross sectional area of explosive column to the cross sectional area of blasthole). This should be minimum as it represents the loss of explosive energy.

The shock wave travels at very high speed (3000-5000 m/s) after passing the crushed zone and sets tangential stresses which produce radial cracks extending upto a distance of 4 to 6 times the charge diameter from the hole (Drukovanyi et al.,1976). The maximum radial strain induced by the longitudinal wave emanated from an explosive charge placed in a blasthole is calculated from the equation given below:

$$\varepsilon_{rmax} = K_c \left(\frac{r}{R} \right)^{k_r} \qquad \text{...(Eqn-1)}$$

Where,

ε_{rmax} = Maximum radial strain of the longitudinal wave
K_c = Scaled strain intercept (a constant depending on the detonating pressure of explosive)
k_r = Rock constant.
r = radius of blasthole (m)
R = Radial distance from blasthole (m)

Further, the shock waves travel upto the nearest free face and get reflected as tensile wave through the rock. Rock being weak in tension fails whenever the tensile stresses exceed the tensile strength of rock. The failure mode is visualized in the form of spalling extending upto the blast hole from where the energy has been initiated(Fig.1). It has been reported that the shock energy, which generates cracks, accounts for only 5 to 15% of total explosive energy(Drukovanyi et al.,1976). This strongly proves that the main cause of rock breakage is due to high gas pressure exerted through the small cracks (blast-induced and natural both) and their enlargement towards the free face. The effect of reflected tensile wave (spalling) joins the cracks developed due to gas pressure.

Crandell (1949) proposed that the damage caused by the blast vibrations was proportional to the energy ratio. The energy ratio, ER, was defined as ratio of the squares of the acceleration, a, and the frequency, f.

$$ER = \frac{a^2}{f^2} \qquad \text{...(Eqn-2)}$$

Langefors et al. (1973), Edwards and Northwood (1960), USBM (1971) and several others proposed particle velocity as a blast damage criteria.

a) There was a common agreement that a PPV of less than 50 mm/s would have low probability of structural damage to residential buildings.

b) There is scarcity of data relating PPV to rock damage in underground openings.

Langefors and Kihlstrom (1973) have proposed the following criteria for tunnels. - PPV's of 305 mm/s and 610 mm / s results in fall of rock in unlined tunnels and formation of new cracks respectively.

Bauer and Calder (1970) observed that no fracturing of intact rock will occur for a PPV of 254 mm/s, PPV of 254 - 635 mm/s results in minor tensile slabbing and PPV of 635 - 2540 mm / s would cause strong tensile and some radial cracking. Break up of rockmass will occur at a PPV of 2540 mm / s.

Holmberg and Persson's (1979) stated that damage is a result of induced strain (ε) which is given by,

$$\varepsilon = V/c \qquad \text{...(Eqn-3)}$$

Where,

V = peak particle velocity and

c = Characteristic propagation velocity of (P/S/Rayleigh wave)

It was also observed by them that the proposed generalized PPV equation is valid only for the distance that are long in comparison to charge length, so that charge can be considered as concentrated. For an extended charge of linear charge concentration l (kg/m), they obtained a first approximation of the resulting PPV by integrating the generalized equation for the total charge length.

$$V = K\, l^{\alpha} \left[\int_0^H \frac{dx}{\left\{D^2 + (D - x)^2\right\}^{\frac{\alpha}{2\beta}}} \right]^{\alpha} \qquad \text{...(Eqn-4)}$$

For arbitrary explosive (not ANFO), weight strength must be made equivalent of ANFO. For competent Swedish bedrock masses the constants used are K = 700, α = 0 .7 and β = 1.5. The computed damage zones is estimated from a plot if V vs. R

Bogdanhoff (1995) monitored near field blast acceleration of an access tunnel in Stockholm. Vibration measurements were done at distances between 0.25 and 1.0 m. outside tunnel perimeter holes with accelerometers. Altogether eight blasts were monitored and the vibrations were filtered and PPV in the assumed damage range was found to be between 2000 and 2500 mm/s.

Blair et al (1996) proposed that Holmberg model warrants further investigation. The Holmberg model assumes that for blast-hole of length, L the vibrations peaks (such as V_1 and V_2) may be numerically added at point P to yield the total peak vibration, V_T. Blair argued that as this model does not incorporate any time lag for the vibration peaks at point P the model is not capable of providing the correct near field analysis. They developed a Dynamic finite element model to assess the damage zone.

Holmberg and Persson (1997) extended the applicability of their model and showed from comparison of theoretical and experimental values that the effective parts of elemental waves arrive at a point almost simultaneously. They, therefore, neglected the difference in time of the arrival of elemental waves from different parts of charge.

3.0 DESIGN OF EXPERIMENT

Most of the damage threshold levels are arrived at using far-field vibration monitoring and extrapolation to near field. To understand the blast-induced damage it is necessary to monitor close to the blast to arrive at ground vibration threshold levels for rock damage. One such monitoring by Bogdanhoff (1995) using uniaxial accelerometers has indicated that the PPV range for rock damage was between 2000 and 2500 mm/s. The PPV levels are too high for the near-field monitoring using ordinary geophones in the underground and hence accelerometer based seismograph (Fig 2) with a monitoring range up to 500g has been put to use in the current study. The high frequency geophone based seismograph and triaxial geophone based seismograph were also used for the cross verification of vibration levels. The insitu rock strength is tested using Schmidt rebound hammer and laboratory testing is also carried out on the cores. To determine the dynamic strength of the rock, P-wave and S-wave velocity are measured using Sonic Viewer. Joint characteristics are also studied in an attempt to determine the RMR (Bieniawski, 1973) and Q-index (Barton et al, 1973). Overbreak for the each blast has been measured using overbreak measuring telescopic rod (Fig 3), designed and fabricated in Indian School of Mines, Dhanbad, under the supervision of the authors.

4.0 FIELD INVESTIGATIONS

4.1 Geology and Geotechnical Investigations

Investigations were carried out in one of the metal mines in eastern India where burn cut is practised on a large scale. Due to higher confinement and inadequate free face the ground vibrations are normally higher irrespective of the best possible delay sequence. A study has been carried out to assess the blast-induced damage to the rockmass. The type of rock is chlorite-sericite-schists of massive metamorphic formation. Some of the geo-technical studies conducted on the rock samples are tabulated in **Table 1.**

Table 1 – Laboratory test results on rock samples

Rock property	Value	Rock Property	Value
R. Q. D.	81.67	Q - Index	5.11
Cohesion strength (MPa)	13.5	UCS of hangwall (MPa)	77.64
Angle of internal friction (Deg.)	41	UCS of ore (MPa)	64.45
Tensile strength of ore (MPa)	10.45	Tensile strength of hangwall (MPa)	10.27
Young's modules of ore (GPa)	35.89	Young's modulus of hangwall (GPa)	28.66
P-wave velocity (km/s)	4.5 – 6.1	Poisson's ratio	0.1 – 0.04
S-wave velocity (km/s)	2.5 – 3.5	R. M. R	66

4.2 Mining Subsystems

The mine has both mechanized and manual faces. The subsystem details of both the faces are described in Table 2.

Table 2 – Details of mining subsystems in mechanized and manual face

<table>
<tr><th colspan="2">Parameters</th><th>Mechanised face</th><th>Manual face</th></tr>
<tr><td colspan="2">Face size</td><td>5×3.2 m</td><td>4×3 m</td></tr>
<tr><td rowspan="5">Drilling</td><td>Diameter of blasthole (mm)</td><td>38</td><td>32</td></tr>
<tr><td>Diameter of reamer hole (mm)</td><td>64</td><td>32</td></tr>
<tr><td>No. of reamer holes</td><td>4</td><td>1</td></tr>
<tr><td>Drilling length (m)</td><td>3.2</td><td>1.6</td></tr>
<tr><td>Machine used for drilling</td><td>Jumbo Drill (4 nos) manufactured by Atlas Copco</td><td>Jack hammer with air leg</td></tr>
<tr><td rowspan="2">Blasting</td><td>Explosive and detonator used</td><td colspan="2">Explosive used: Powergel 801, Nobel gel, Belmx, Indorock
Short and long delay detonators manufactured by Indian Explosive Ltd. are used. Each increment in short delay number increase a delay time of 25ms whereas for long delay it is 300ms.</td></tr>
<tr><td>Short and long delay used</td><td>As shown in Fig-4</td><td>As shown in Fig-5</td></tr>
<tr><td rowspan="2">Loading and transport</td><td>Mucking</td><td>LHD and Scoop Tram</td><td>Rocker shovel</td></tr>
<tr><td>Transportation</td><td>Mine truck of 25t capacity or Low Profile dump truck of 10t capacity dumped in ore pass or directly in stope for filling</td><td>Tub of 0.6m^3 capacity hauled by battery locomotive.</td></tr>
<tr><td>Support</td><td colspan="3">The suggested support system used in the mine is rock bolting. Rock bolts are used as the permanent support for the drifts and declines and as well as for raise and winze.
For drift/decline: 1.6m × 1.6m direction of bolt is perpendicular to dip of rock.
Length of bolt = 1.6 m 32 mm dia with twisted surface.
Shotcrete/grouting mixture: - 1:1:0.5 (cement: sand : water)
Strength of bolt: - 16 ton
Maximum distance of row of support from face = 2.5m
Large permanent excavation/junctions: - 1.2m × 1.2m</td></tr>
</table>

The charging pattern for the mechanized drifts is described in Table 3 and Fig.4.

Table 3 - Charging pattern of mechanised drift (4.5 m x 3.2 m)

Hole(s)	Delay No.	No. of Holes	Charge/Hole (Cartridge)	Total Charge (Cartridge)
Center hole	0	1	10 + 1P	11
1st square	1, 2, 5, 8	4	10 + 1P	44
2nd square	II x 4, III×4	8	11+ 1P	96
3rd square	IV x 4, V×4	8	11 + 1P	96
Easers	VI x 6, VII×3	9	12 + 1P	117
Side holes	VIII×6	6	11+1P	72
Top holes	IX x 8	8	10 + 1P	88
Bottom holes	X x 8	8	12 + 1P	104
Total		52		628
Depth of round: 3.2 m Dia. of blasting holes: 38 mm Dia. of reamer holes: 64 mm Total no. of cartridges: 628			Dia of cartridge: 32 mm Wt. of cartridge: 0.220 kg. Total explosive: 138.16 kg. Total Yield: 157.5 t (expected)	

The charging pattern for the manual face is described in Table 4 and Fig. 5.

Table 4 - Charging pattern of manual face (4 m x 3 m).

Hole(s)	Delay No.	No. of Holes	Charge/Hole (Cartridge)	Total Charge (Cartridge)
Center hole	Reamer(R)	1	0	0
1st square	I×4, II×4	8	4 + 1P	40
2nd square	III×4, IV×4	8	4 + 1P	40
Easers	V×4, VI×4, VII×4	12	5 + 1P	72
Side holes	VII×2, VIII×4	6	5 + 1P	36
Top holes	VII×1, IX×2, X×2	5	4 + 1P	25
Bottom holes	VII×1, IX×2, X×2	5	6 + 1P	35
Total		44+1		248
Depth of round: 1.6 m Dia. of blasting holes: 32 mm Dia. of reamer holes: 32 mm Total no. of cartridges: 248			Dia of cartridge: 25 mm Wt. of cartridge: 0.125 kg. Total explosive: 31 kg. Total Yield: 53.76 t (expected)	

4.3 GROUND VIBRATION MEASUREMENTS AND ANALYSIS

Blast-induced acceleration measurement has been done using accelerometer of 500g range manufactured by Instantel Inc. Canada, for the first time in India. PPV has also been monitored using Minimate 077 of the same manufacturer. The monitored accelerations have been integrated to achieve DPPV (here in after referred as derived PPV). Scaled distance of the each blast has been calculated using the formula (Eqn-5) proposed by Ambraseys and Hendron (1968).

$$SD = \frac{R}{\sqrt[3]{W}} \qquad \text{...(Eqn-5)}$$

Where, SD = Scaled Distance

R = Distance of instrument from blast (m)

W = Maximum charge per delay (kg)

Regression analysis has been carried out between the scaled distance and acceleration (Fig. 6). The predictor equation found has a correlation coefficient of 0.84 and is given below:

$$a = 24.315 \times \left(\frac{R}{\sqrt[3]{W}} \right)^{-0.8711} \qquad \text{...(Eqn-6)}$$

Where, a = Acceleration (g)

Similarly the best-fit curves for derived PPV (Fig. 7 and Eqn-7 with correlation coefficient of 0.78) and for actual PPV monitored in the field (Fig 8 and Eqn-8 with correlation coefficient of 0.66) are established and are presented here:

$$DPPV = 260.76 \times \left(\frac{R}{\sqrt[3]{W}} \right)^{-0.8937} \qquad \text{...(Eqn-7)}$$

Where, DPPV = PPV derived from acceleration by integration (mm/s)

$$V = 339.25 \times \left(\frac{R}{\sqrt[3]{W}} \right)^{-1.1574} \qquad \text{...(Eqn-8)}$$

Where, V = Actual PPV measured in the field (mm/s)

It is clear from the above analysis that acceleration measurement is more accurate and dependable in predicting the maximum explodable charges in tunnel blasting for minimizing overbreak.

4.4 OVERBREAK PREDICTION

The acceleration and PPV threshold levels, for the actual overbreak measured in the tunnel which is 0.4m, have been derived from each vibration predictor and are shown in Fig 9. The damage threshold level for acceleration is found to be around 145.03 g and for derived PPV (DPPV) arrived by integration of acceleration is 1628.97 mm/s. on the contrary the damage threshold level using the extrapolated PPV, indicates a value of 3638.89 mm/s, which is comparatively higher than the earlier reported values of Bogdanoff (1995). However, the derived PPV value is observed to be well within the suggested range. It is also seen that predicting blast damage using acceleration measurements would result in arriving at accurate maximum charge per delay values due to higher correlation coefficient obtained in comparison to far-field PPV measurements and derived PPV (DPPV) values.

The roof holes are drilled 0.15 m below the desired excavation level. Therefore, theoretically, maximum charge per delay to be used in roof holes for zero overbreak, can be estimated using the suggested vibration predictors. The percentage overbreak at different maximum charge per delay has been shown in Fig 10. The same may be used to fix the overbreak to a desired level. The study concludes that the maximum charge per delay, computed from acceleration measurements, to obtain zero overbreak as 2 kg while using PPV measurements the suggested maximum charge per delay as 0.75 kg.

5.0 CONCLUSION

The existing criteria for rock damage assessment based on ground vibration have been reviewed. Laboratory testing of rock and trial blasts in the mine have been carried to study the blast- induced damage in burn cuts. The acceleration and PPV have been monitored for each blast. The measured accelerations have been carefully integrated to arrive at the corresponding PPVs. The vibration predictors for the acceleration, derived PPV and measured PPV have been established. Vibration predictor derived from the near-field acceleration monitoring has the maximum correlation coefficient indicating the inter-dependability and consistency. The threshold levels for damage/overbreak has been established and is found to be around 145.03g for acceleration, 1628.97 mm/s for derived PPV, 3638.89mm/s for measured PPV. The measured PPV is of far field in nature and hence, may be unsuitable for determination of damage threshold level. Acceleration measurement in the near field is the better choice for damage prediction. It is necessary to include more observations before suggesting a definite relationship.

ACKNOWLEDGEMENT

This paper forms a part of the research and development project on “Development of Predictive Models for Blast-Induced Rock Damage Assessment (BIRD) in Tunnels” sponsored by Ministry of Human Resource Development, Government of India. The authors are grateful to MHRD for sanctioning the project. The authors are also thankful to Director, Indian School of Mines, Dhanbad and Head, Department of Mining Engineering for providing the all the facilities and encouragement for writing this paper. The authors gratefully acknowledge the wholehearted help provided by the mine officials during the field investigations.

REFERENCES

Ambraseys N.R. and Hendron A.J. (1968), “Dynamic behavior of rockmasses”, Rock Mechanics in Engineering Practices, (Eds) Stagg K.G. and Zienkiewiez O.C., John Willey and Sons, London, pp 203-207.

Barton N., Lien R. and Lunde J. (1974), “Engineering classification of rock for the design of tunnel support”, Norwegian Geotechnical Institute, Publication No. 106, Oslo, pp 1-115.

Bieniawski Z.T. (1973), “Engineering classification of jointed rockmasses”, Transaction South African Institution of Civil Engineers, Vol 15, pp 335-344.

Blair Dane and Minchinton Alan (1996), “On the damage zone surrounding a single blasthole”, Proceedings of Rock fragmentation by blasting, FRAGBLAST-5, (Ed) Mohanty, Montreal, Quebec, Canada, 23-24 August, pp121-130.

Bogdanoff Ingvar (1995), “Vibration measurements in damage zone in tunnel blasting”, Proceedings of Rock fragmentation by blasting, FRAGBLAST-5, (Ed) Mohanty, Montreal, Quebec, Canada, 23-24 August, pp177-185.

Drukovanyi M. F., Kravtsov V. S., Chernyavskii, E Yu, Shelenok V.V., Reva N.P. and Zver’kov S. N. (1976), “Calculation of fracture zones created by exploding cylindrical charges in ledge rocks”, Soviet Mining Science, Vol.12(3) May – June, pp. 292-295.

Edwards A.T. and Northwood T.D. (1960), “Experimental studies of effects of blasting on structures”, The Engineer, 211.

Holmberg R. and Persson P.A. (1979), “ Swedish approach to contour blasting”, Proceedings of Fourth Conference on explosive and blasting techniques, pp113-127.

Holmberg R. and Persson P.A. (1997), “ The relation between strain energy, rock damage, fragmentation and throw in rockblasting”, Proceedings of Rock fragmentation by blasting, FRAGBLAST-5, (Ed) Mohanty, Montreal, Quebec, Canada, 23-24 August, pp.

Gustafsson R. (1973), “Swedish Blasting Technique”, SPI Gothenburg, Sweden, pp 77 - 143.

Jimeno C. L., Jimeno E. L. and Carcedo F.J.A. (1995), “Drilling and Blasting of Rocks”, A. A. Balkema, Rotterdam, Brookfield Publication, pp 200-287.

Langefors U. and Kihlstrom B. (1973), “The Modern Techniques of Rock Blasting”, John Wiley and sons, pp 34 - 73.

Murthy V.M.S.R. and Dey K. (2002), “Development of Predictive Models for Blast-Induced Rock Damage Assessment (BIRD) in Tunnels”, Interim Report, MHRD Project No: MHRD (27)/99-00/111/ME, pp 12-43.

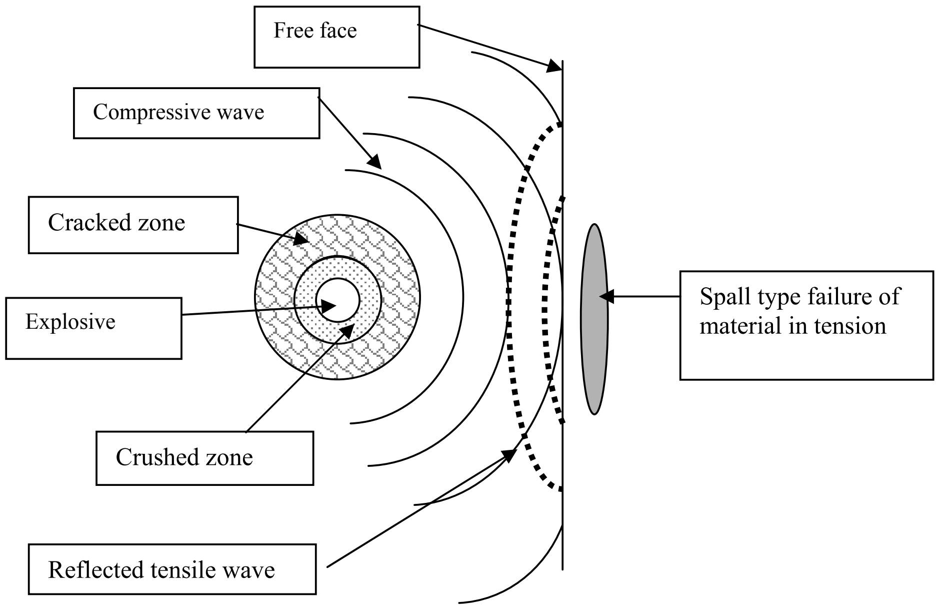

Figure 1: Wave propagation and spalling in presence of free face

Fig. 2- Accelerometer based seismograph with accessories, Instantel Make

Fig. 3- Overbreak measuring telescopic rod, designed and fabricated in ISM, Dhanbad

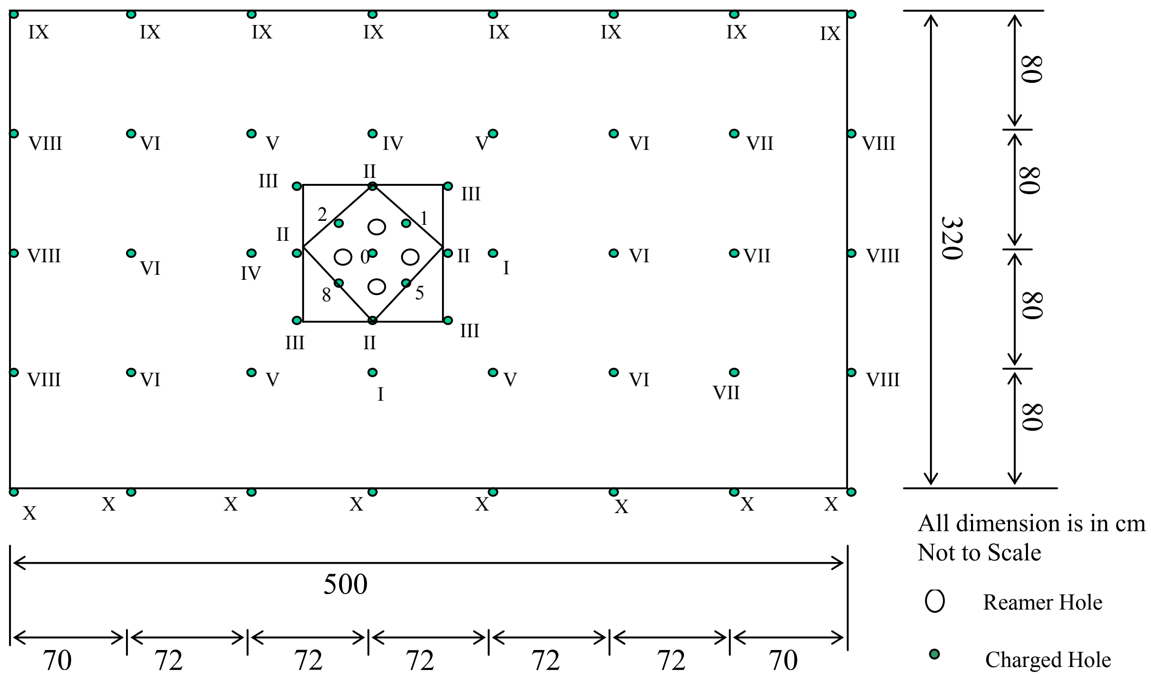

Fig 4 - Blast pattern for drift with mechanised drilling

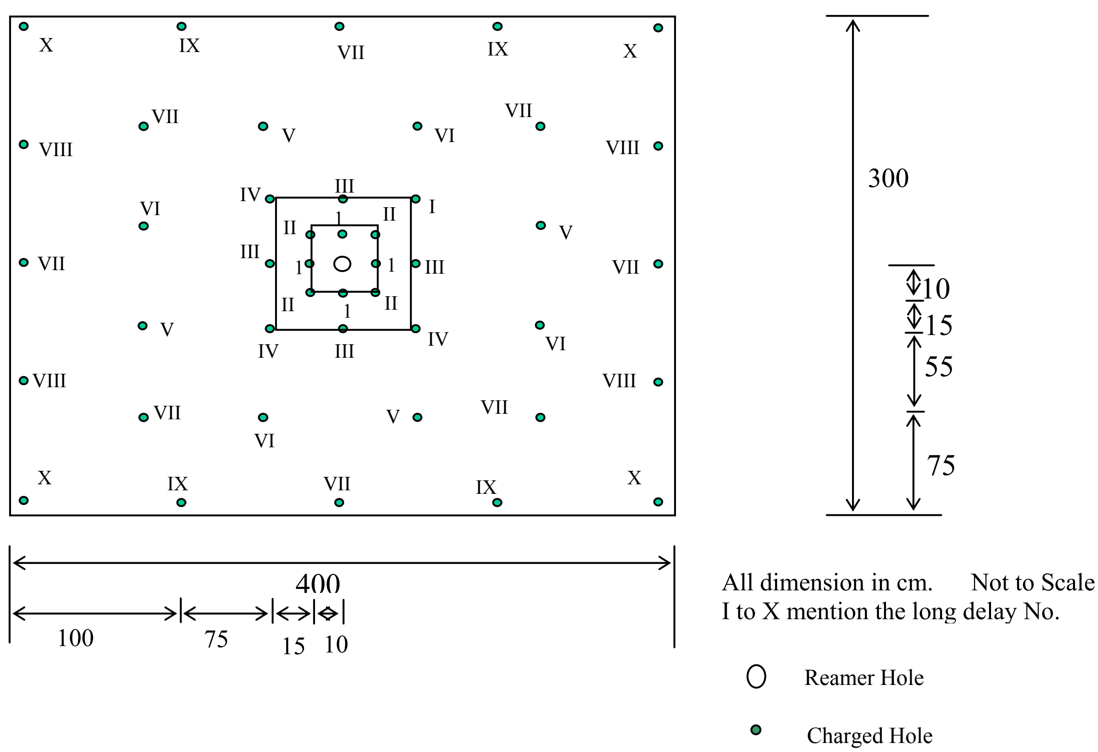

Fig 5 - Blast pattern for drift with manual drilling

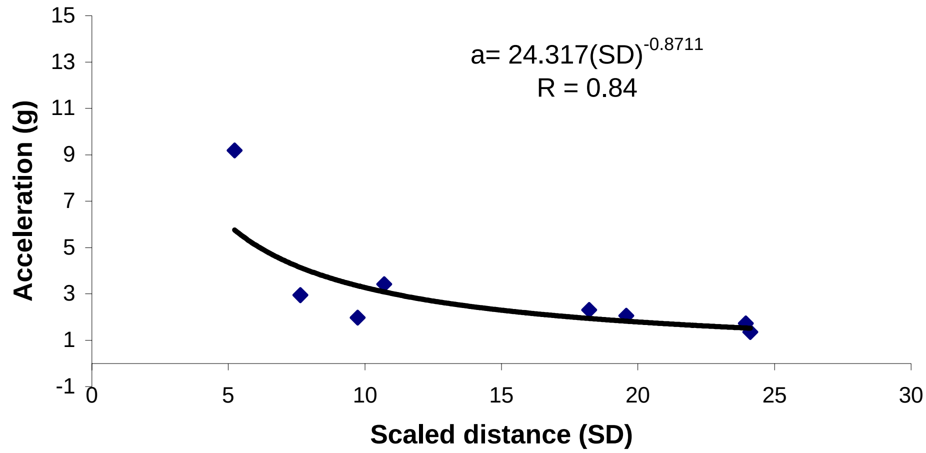

Fig 6: Acceleration predictor in horizontal drift

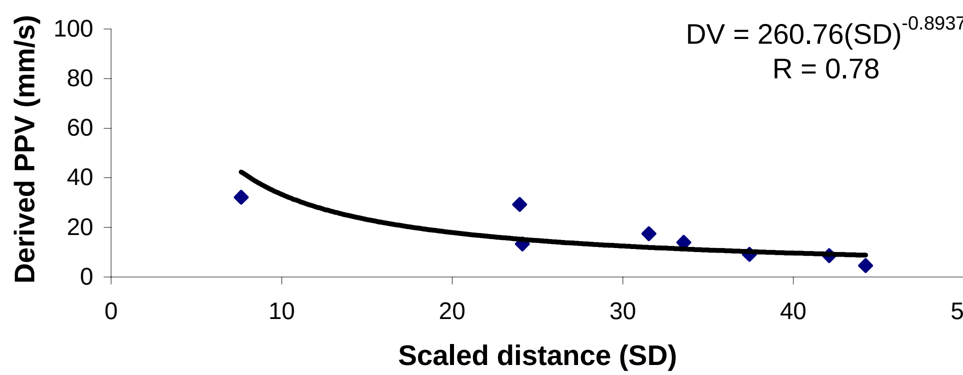

Fig 7: PPV predictor derived from acceleration measurements

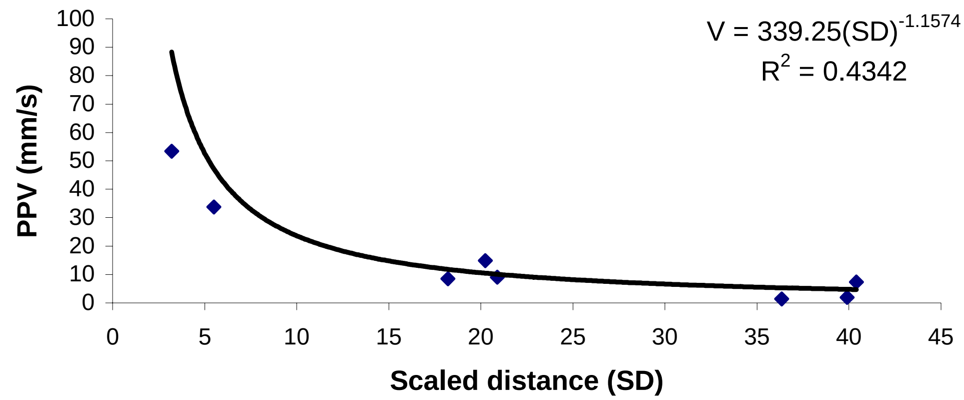

Fig 8: PPV predictor in horizontal drifts from measured PPV

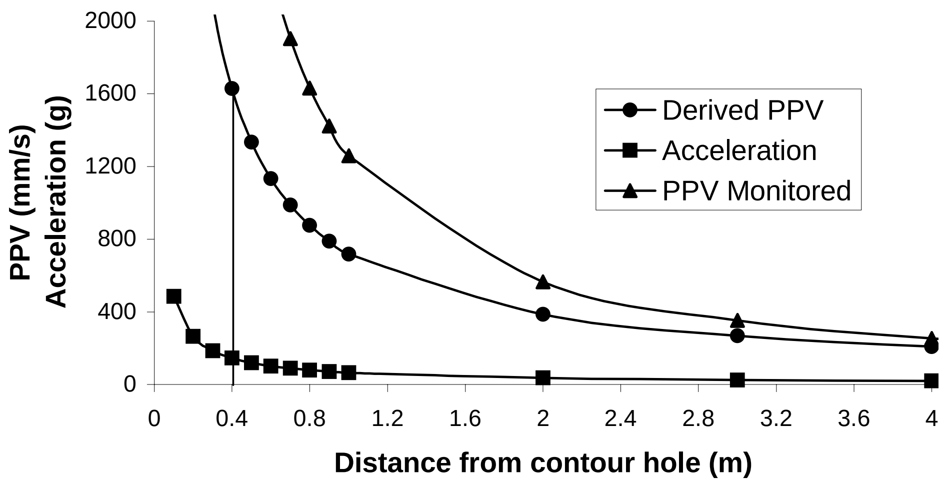

Fig 9: Overbreak threshold levels

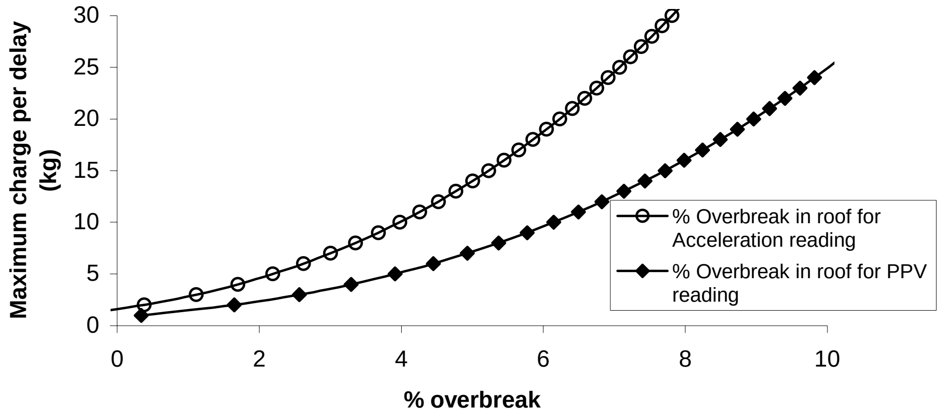

Fig 10: Determination of Maximum charge per delay for controlling overbreak